Applied Catalysis B: Environmental 125 (2012) 1–9

Contents lists available at SciVerse ScienceDirect

Applied Catalysis B: Environmental

journal homepage: www.elsevier.com/locate/apcatb

Monometallic Pd/Fe_3O_4 catalyst for denitrification of water

Wuzhu Sun[a,b], Qi Li[a,*], Shian Gao[a], Jian Ku Shang[a,c]

[a] Materials Center for Water Purification, Shenyang National Laboratory for Materials Science, Institute of Metal Research, Chinese Academy of Sciences, Shenyang 110016, PR China
[b] University of Science and Technology of China, PR China
[c] Department of Materials Science and Engineering, University of Illinois at Urbana-Champaign, Urbana, IL 61801, USA

ARTICLE INFO

Article history:
Received 30 November 2011
Received in revised form 18 April 2012
Accepted 15 May 2012
Available online 22 May 2012

Keywords:
Pd/Fe_3O_4
Catalytic denitrification
Superparamagnetic catalyst
Fe(II)/Fe(III) redox couple

ABSTRACT

A magnetite supported monometallic Pd catalyst was synthesized by a co-precipitation process followed with the reduction in pure hydrogen at 453 K. The catalyst was composed of ultrafine Pd nanoparticles (~2 nm) highly dispersed on the surface of superparamagnetic Fe_3O_4 nanoparticles. Aside from its roles as the catalyst support and the magnetic separation medium, Fe_3O_4 was found to be a good promoter for the nitrate reduction, where nitrate was firstly reduced to nitrite by the Fe(II)/Fe(III) redox couple, and subsequently reduced to nitrogen and ammonium. Further mechanistic studies demonstrated that besides the Pd sites, active sites for the nitrite reduction also exist on the surface of Fe_3O_4. Part of the nitrite reduction occurred on the surface of Fe_3O_4, which may also be attributed to the Fe(II)/Fe(III) redox couple. In the present study, ammonium was the main product because of the different denitrification mechanisms compared with bimetallic catalysts.

1. Introduction

Due to the intensive agricultural activities, especially over-fertilization, nitrate concentrations in both surface and ground water have increased in many locations throughout the world, and the problem is becoming increasingly important with the fast increase of agricultural and industrial activities in recent years [1–3]. Because of its widespread presence and toxicity, nitrate becomes one of the most common groundwater contaminants in many countries. Nitrate could cause various problems to the health of human beings, such as blue baby syndrome, high blood pressure, diabetes, and liver damage. It is also the precursor of nitrosamine, which could cause various cancers [3–8]. Therefore, the World Health Organization (WHO) recommended that the maximum contaminant level (MCL) for nitrate in drinking water should be below 50 ppm [9], and many countries have formulated their own MCLs according to their domestic conditions.

Many treatment methods have been proposed to remove nitrate from contaminated water, including both biological and physical chemical denitrification approaches [10–15]. Among various physical–chemical denitrification processes, such as ion exchange, reverse osmosis, electrodialysis and catalytic reduction by hydrogen or other reducing agents, the catalytic reduction by reducing agents had been considered as one of the most promising methods to treat nitrate in water [16–19]. Since Vorlop and Tacke [20] demonstrated for the first time that the catalytic reduction of nitrate by reducing agent was achievable, extensive research efforts have been made in this approach [16–33].

Most catalysts for the nitrate reduction are composed of a noble metal and a promoter, which may be a transition metal or a metal oxide. The function of the promoter is to reduce nitrate to nitrite by a redox process to start the catalytic process, while the noble metal plays an important role in maintaining transition metal in metallic state and reducing nitrite by activated hydrogen [3,16–18]. Currently, most research efforts are focused on bimetal denitrification catalysts, in which the noble metals usually are Pd, Pt, Ru, Rh, or Ir, and the promoters are Cu, Sn, Ag, or In [16–29]. By comparison, a limited number of studies have been conducted in noble metal/metal oxide denitrification catalysts, in which a metal oxide acts as the promoter. Till now, only CeO_2, TiO_2, and SnO_2 were found to be good promoters of the noble metal in the denitrification process [3,30–33]. Based on the current understanding of the catalytic denitrification mechanism, it appears that any catalyst associating a noble metal, capable of chemisorbing hydrogen, with a component, having a redox behavior may catalyze nitrate reduction [33]. Thus, novel catalyst material systems for denitrification could be developed by following this approach, and by incorporating other functions to enhance water treatment performance in engineering devices.

Because of its easy separation from an aqueous environment under the external magnetic field, the utilization of magnetic magnetite (Fe_3O_4) has been explored for various water treatment applications, for example, dehalogenation, heavy metal ion

* Corresponding author at: 72 Wenhua Road, Shenyang, Liaoning Province 110016, PR China. Tel.: +86 24 83978028; fax: +86 24 23971215.
E-mail address: qili@imr.ac.cn (Q. Li).

0926-3373/$ – see front matter © 2012 Elsevier B.V. All rights reserved.
http://dx.doi.org/10.1016/j.apcatb.2012.05.014

adsorption, and pesticide removal [34–37]. Since both Fe(II) and Fe(III) ions are present in the oxide, electrons could exchange between them under certain conditions. Thus, it may provide the redox function needed in the catalytic denitrification. In this study, a novel magnetite supported monometallic Pd denitrification catalyst was synthesized by a co-precipitation process followed with the reduction in pure hydrogen at 453 K. Besides the roles as the catalyst support and the magnetic separation medium, denitrification results demonstrated that Fe_3O_4 was a good promoter for nitrate reduction. Further mechanism studies suggested that besides the Pd sites, there were also active sites on the surface of Fe_3O_4 for the nitrite reduction. Nitrate was firstly reduced to nitrite by the Fe(II)/Fe(III) redox couple, and subsequently reduced to nitrogen and ammonium. Consequently, the new catalysts demonstrate fast denitrification performance in water solution. Because of the difference in the denitrification mechanism, the main reduction product was ammonia as opposed to the more toxic nitrite produced with some of the bimetallic catalysts.

2. Experimental

2.1. Materials and chemicals

All chemicals are reagent grade and used without further purification. $FeCl_3{\cdot}6H_2O$, $PdCl_2$, Na_2CO_3, $NaNO_3$, NH_4Cl, KOH and HCl were obtained from Sinopharm Chemical Reagent Corporation (Shanghai, P.R. China). $NaNO_2$ was obtained from Tianjin Kermel Chemical Reagents Development Center (Tianjin, P.R. China). Deionized (DI) water (18.2 MΩ) was used in all experiments. All the gases used in the experiment have the high pure degree (99.99%). Ar and CO_2 gases were obtained from Dalian DaTe gas Corp. Ltd. (Dalian, P.R. China), and H_2 gas was obtained from the Guangzheng hydrogen generator (Guangzheng analytical Instruments Corp. Ltd. Shenyang, P.R. China). Nitrate (16.1 mM) and nitrite (21.7 mM) stock solutions (1 g/L NO_3^- or NO_2^-) were prepared by dissolving proper amounts of $NaNO_3$ and $NaNO_2$ into DI water, respectively, and stored in the dark in a refrigerator at 277 K.

2.2. Preparation of magnetite supported monometallic Pd catalyst

Co-precipitation method was used to prepare the Pd/Fe_3O_4 catalyst precursor [38,39]. 3.5 g $FeCl_3{\cdot}6H_2O$ and 0.05 g $PdCl_2$ was dissolved in 18 mL DI water under magnetic stirring at room temperature. After the mixture solution became clear, 1.0 M Na_2CO_3 solution was added dropwise to the mixture solution until its pH reached 9. After being stirred for 3 h, the precursor solution was then aged for 3 h before the precipitated precursor (denoted as $PdO/Fe(OH)_x$) was removed from the solution and then thoroughly washed and dried. The Pd/Fe_3O_4 catalyst was obtained by the reduction of $PdO/Fe(OH)_x$ precursor in a flow of pure hydrogen at 453 K. The nominal Pd content for Pd/Fe_3O_4 catalyst was 3%.

2.3. Catalyst characterization

The X-ray diffraction (XRD) patterns of both $PdO/Fe(OH)_x$ and Pd/Fe_3O_4 catalyst were obtained by a D/MAX-2004 X-ray powder diffractometer (Rigaku Corporation, Tokyo, Japan) with Ni-filtered Cu (λ = 0.15418 nm) radiation at 56 kV and 182 mA. X-ray photoelectron spectroscopy (XPS) measurements were conducted with an ESCALAB250 X-ray Photoelectron Spectrometer (Thermo Fisher Scientific Inc., Waltham, MA, U.S.A.) with an Al K anode (1486.6 eV photon energy, 300 W). The microstructure of Pd/Fe_3O_4 catalyst was examined by the transmission electron microscopy (TEM) on a JEOL 2010 transmission electron microscope (JEOL Ltd., Tokyo, Japan) operating at 200 kV. TEM samples were prepared by dispersing Pd/Fe_3O_4 catalyst powder in ethanol, applying a drop of the dispersion on a Cu grid, and drying in air at 60 °C for 3 h. The particle size distribution of Pd/Fe_3O_4 catalyst was determined by the dynamic light scattering method with a Malvern Zetasizer (Nano-zs90, Malvern Instruments Ltd., Malvern, Worcestershire WR14 1XZ, UK). Zeta-potential value of Pd/Fe_3O_4 catalyst at different pH was measured by an electrophoretic spectroscope (JS84H, Shanghai Zhongchen Digital Instrument Co., Ltd., Shanghai, P.R. China). The zeta-potential measurement samples were prepared by mixing 100 mg Pd/Fe_3O_4 catalyst powder with 200 mL 0.01 M KNO_3 solution, and their pH values were adjusted between 3 and 10 by adding 0.1 M HNO_3 or 0.1 M KOH. The magnetic measurements were carried out in a superconducting quantum interference device magnetometer at 298 K (Quantum Design MPMS-7, Quantum Design, Inc. USA). Nitrogen adsorption–desorption measurement was performed with an Autosorb-1 Analyzer (Quantachrome Instruments, Boynton Beach, FL, U.S.A.). The specific surface area was calculated using the standard Brunauer–Emmett–Teller (BET) method, and the mesopore size distributions were obtained by the Barrett–Joyner–Halenda (BJH) method from the desorption branch data of nitrogen adsorption isotherm.

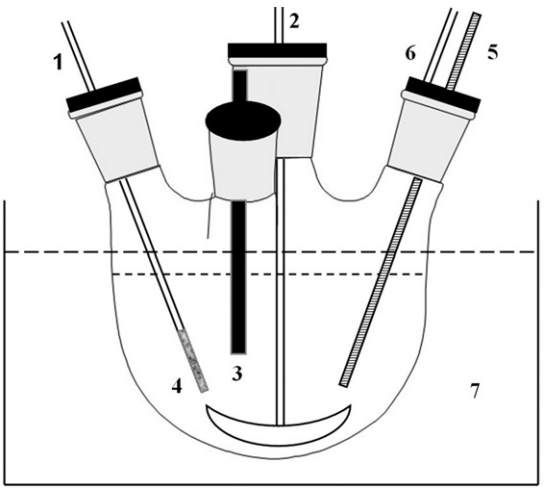

Fig. 1. The schematic diagram of the reactor: (1) gas inlet, (2) mechanical agitator, (3) pH meter, (4) porous glass tube, (5) thermometer, (6) gas outlet, and (7) water bath.

2.4. Catalytic denitrification experiment

All the catalytic reduction experiments of nitrate and nitrite were conducted in a 250 mL glass reactor equipped with a mechanical agitator and a pH meter, which is schematically demonstrated in Fig. 1. In a typical setup, 0.1 g Pd/Fe_3O_4 powder was loaded into the reactor with 180 mL deionized water under vigorously stirring, and Ar was fed into the reactor from its bottom. After being purged with Ar for 30 min, 20 mL nitrate (16.1 mM) or nitrite (21.7 mM) solution was added into the reactor, and then the gas was changed to H_2 for the catalytic denitrification. In these experiments, the solution pH was controlled in three different ways, respectively: (1) co-feeding CO_2 with H_2 during the reaction, (2) just adjusting the initial solution pH with 0.1 M HCl and 0.1 M KOH, and (3) maintaining a constant pH with 0.1 M HCl addition during the reaction. During the experiment, 5 mL suspension was withdrawn at the regular time interval. Then, we applied an external magnetic field to separate the catalyst from the suspension, and use the clear solution to determine the concentrations of N-species. The concentration of NO_3^-, NO_2^-, and NH_4^+ were determined by the ion chromatograph (Dionex ICS 1100 Ion Chromatography with a conductivity cell). The Dionex AS-22 column was used to determine the concentrations of NO_3^- and NO_2^- (4.2 mM carbonate and 1.4 mM bicarbonate buffer

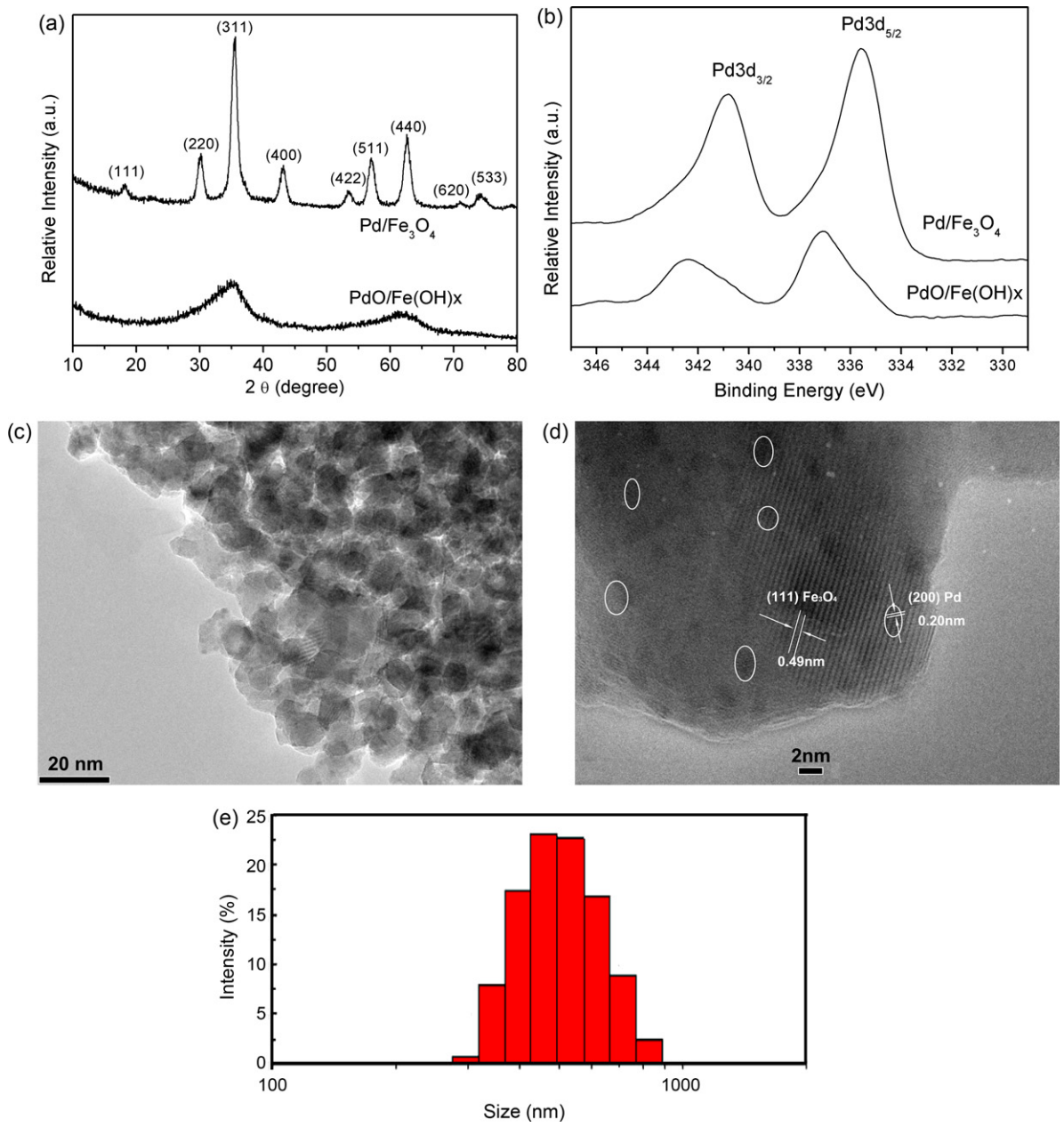

Fig. 2. (a) The X-ray diffraction pattern of the Pd/Fe_3O_4 catalyst, compared with that of the $PdO/Fe(OH)_x$ precursor. (b) High-resolution XPS scan over Pd 3d peaks of the Pd/Fe_3O_4 catalyst, compared with that of the $PdO/Fe(OH)_x$ precursor. (c) and (d) HRTEM images of the Pd/Fe_3O_4 catalyst. (e) The particle size distribution of the Pd/Fe_3O_4 catalyst.

solution as the effluent), while the Dionex CS12A column was used to determine the concentration of NH_4^+ (20 mM methanesulfonic acid as the effluent). All catalytic denitrification experiments were conducted at room temperature (293 K) and atmospheric pressure, and the initial activity of the catalyst was evaluated using the specific removal rate of nitrate within the initial 10 min reaction time. The catalyst performance was evaluated by calculating the nitrate conversion ($X_{NO_3^-}$), the selectivity to nitrite ($S_{NO_2^-}$), and the selectivity to ammonium ($S_{NH_4^+}$) as following equations, respectively [40]:

$$X_{NO_3^-} = \frac{n_{iNO_3^-} - n_{NO_3^-}}{n_{iNO_3^-}} \quad (1)$$

$$S_{NO_2^-} = \frac{n_{NO_2^-}}{n_{iNO_3^-} - n_{NO_3^-}} \quad (2)$$

$$S_{NH_4^+} = \frac{n_{NH_4^+}}{n_{iNO_3^-} - n_{NO_3^-}} \quad (3)$$

3. Results and discussion

3.1. Physicochemical properties of the Pd/Fe_3O_4 catalyst

Fig. 2a shows the XRD pattern of the Pd/Fe_3O_4 catalyst, compared with that of the $PdO/Fe(OH)_x$ precursor. Before the H_2 reduction process, no obvious diffraction peak could be observed for the $PdO/Fe(OH)_x$ precursor, indicating its amorphous state. After being reduced by H_2, all the diffraction peaks could be attributed to Fe_3O_4 (JCPDS 19-0629), indicating the crystallization process occurred during the reduction process. The Fe_3O_4 crystallite size in the Pd/Fe_3O_4 catalyst is about 10 nm, obtained

from the strongest XRD peak (at $2\theta \sim 36^\circ$) by the Scherrer's formula [41]:

$$D = \frac{0.9\lambda}{\beta \cos \theta} \quad (4)$$

where λ is the average wavelength of the X-ray radiation, β is the line-width at half-maximum peak position, and θ is the diffracting angle. No diffraction peak belonging to Pd could be found in the XRD patterns of Pd/Fe_3O_4 catalyst, indicating that the size of Pd might be very small and they should be highly dispersed in the Pd/Fe_3O_4 catalyst [39].

To examine the existence and state of Pd species in the $PdO/Fe(OH)_x$ precursor and Pd/Fe_3O_4 catalyst, an XPS investigation was conducted to obtain semi-quantitative data on the compositions. High-resolution XPS scan over Pd 3d (Figure 2b) peaks shows that the binding energy of Pd $3d_{5/2}$ is ~337.0 eV for the $PdO/Fe(OH)_x$ precursor, which could be attributed to PdO species as expected. After H_2 reduction process, however, the binding energy of Pd $3d_{5/2}$ shifts to ~335.5 eV, which could be attributed to metallic Pd and indicate the switch of Pd species from PdO to Pd during the reduction process [42]. Thus, XRD and XPS results revealed that the composition of the obtained catalyst is Pd/Fe_3O_4.

To further examine the morphology and the existence of metallic Pd in the Pd/Fe_3O_4 catalyst, TEM observations were made on the Pd/Fe_3O_4 catalyst powder. Fig. 2c shows a representative TEM image of the Pd/Fe_3O_4 catalyst, which demonstrates that the Pd/Fe_3O_4 catalyst consists of agglomerated crystallized nanoparticles with the size of ~10 nm. This observation is consistent with the XRD result. Fig. 2d shows the high resolution TEM (HRTEM) image of the Pd/Fe_3O_4 catalyst, in which two sets of lattice planes could be clearly identified. The larger grain has the inter-planar spacing of ~0.49 nm, corresponding to the (1 1 1) plane of Fe_3O_4. Next to the larger grain, several much smaller grains (2 nm or smaller) exist with the inter-planar spacing of ~0.20 nm, corresponding to the (1 1 1) plane of Pd. Thus, HRTEM observation demonstrates that the Pd/Fe_3O_4 catalyst was composed of highly dispersed ultrafine metallic Pd nanoparticles on the surface of Fe_3O_4 nanoparticles. Due to the ultrafine grain size, the XRD diffraction peak of Pd could not be identified in the XRD pattern of Pd/Fe_3O_4 catalyst. Fig. 2e shows the particle size distribution of these agglomerated nanoparticles. The average size is ~500 nm, and the particle size varies from ~300 nm to 900 nm. The nitrogen adsorption–desorption measurement demonstrated that the Pd/Fe_3O_4 catalyst had a specific surface area of 99.5 m^2/g and an average pore diameter of 6.6 nm.

The electrostatic state of the catalyst surface could largely affect the interaction between ions and the catalyst in an aqueous environment. Fig. 3a demonstrates the zeta-potential measurement results at different pH of the Pd/Fe_3O_4 catalyst. The isoelectric point (IEP) was found at ~pH 5.8. Thus, the surface of Pd/Fe_3O_4 catalyst is positively charged when the solution pH is less than 5.8, and it is negatively charged when the solution pH is over 5.8. Consequently, when the solution pH is less than 5.8, the negatively charged NO_3^- and NO_2^- should be attracted to the positively charged Pd/Fe_3O_4 catalyst, which will be beneficial to their catalytic denitrification.

Fig. 3b demonstrates the magnetic field-dependent behavior of the Pd/Fe_3O_4 catalyst obtained at room temperature. It shows a typical superparamagnetic behavior with zero remanence and zero coercivity [43,44], which could be attributed to the Fe_3O_4 nanoparticle size just at ~10 nm (lower than critical size for its superparamagnetism at ~30 nm) [45]. The saturation magnetization, M_s, could be obtained by extrapolating the graph of M vs. $1/H$ to $1/H \rightarrow 0$ (for $H > 10$ kOe), which was determined at ~75.9 emu/g. Its superparamagnetic behavior and high saturation magnetization are very beneficial to both its good dispersion/redispersion in the aqueous environment and its easy magnetic separation from treated water body afterwards [46]. Unlike the commonly used magnetic particles in water treatment, its superparamagnetic behavior avoids the magnetic attraction between these nanoparticles when there is no external magnetic field, which will enhance their dispersion and contact with ions in the water body. After the water treatment, however, its high saturation magnetization ensures an easy magnetic separation from water when an external magnetic field is present. From above physicochemical characterization results, it is clear that Fe_3O_4 nanoparticles serve as both the catalyst support and a desirable magnetic separation medium in the Pd/Fe_3O_4 catalyst system.

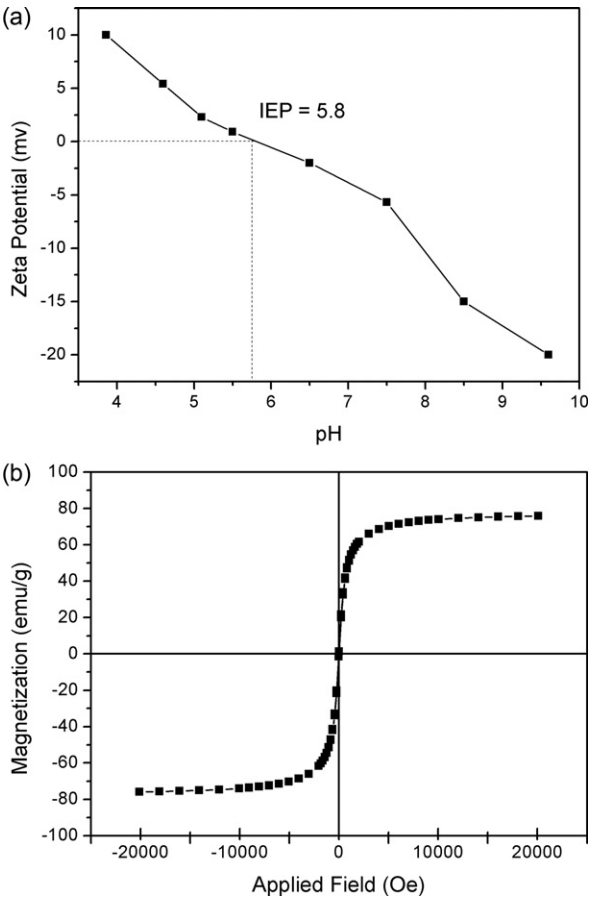

Fig. 3. (a) Zeta-potential measurement result of the Pd/Fe_3O_4 catalyst. (b) Room-temperature magnetization curve of the Pd/Fe_3O_4 catalyst.

3.2. Catalytic reduction of nitrate and nitrite by Pd/Fe_3O_4

Diffusion limitation is a very important factor for the three-phase (solid–liquid–gas) catalytic reaction [47]. Tests were conducted to estimate the effect of the diffusion limitation by varying flow rate of hydrogen, dose of catalyst, and stirring speed. These factors were found to show little effect on the reduction rate of nitrate/nitrite, which suggested that the external diffusion limitation was not significant under the current experimental setup. As suggested in literature [48–51], the internal diffusion limitation could be excluded when the catalyst particle size was below a critical value (usually at tens of microns). Because the particle size of the Pd/Fe_3O_4 catalyst was less than 1 μm, the internal diffusion limitation could also be excluded in our study.

The activity and selectivity of Pd/Fe_3O_4 catalyst for the reduction of nitrate and nitrite were firstly examined on 100 ppm NO_3^- (1.61 mM) and NO_2^- (2.17 mM) solutions with the initial solution pH of ~7.0, respectively, and no pH adjustment was made in the denitrification process. Fig. 4a shows the reduction result

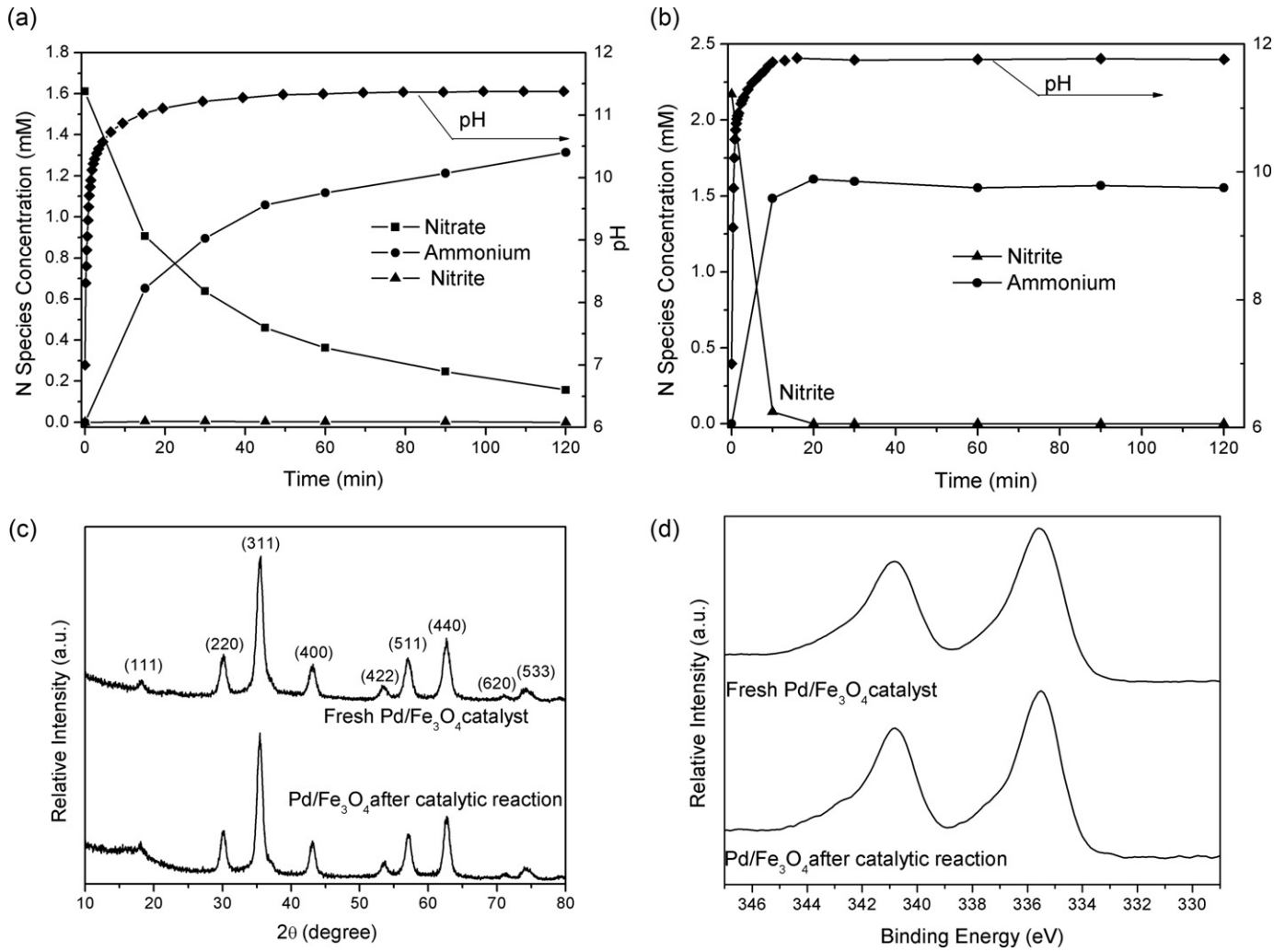

Fig. 4. (a) The time-dependent variations of the concentrations of nitrate, nitrite, and ammonium, and the solution pH during the nitrate reduction process. (b) The time-dependent concentration changes of nitrite and ammonium, and the solution pH during the nitrite reduction process. (c) The X-ray diffraction pattern of the Pd/Fe_3O_4 catalyst magnetically collected after the nitrate reduction experiment, compared with that of the fresh Pd/Fe_3O_4 catalyst. (d) High-resolution XPS scan over Pd 3d peaks of the Pd/Fe_3O_4 catalyst magnetically collected after the nitrate reduction experiment, compared with that of the fresh Pd/Fe_3O_4 catalyst.

of nitrate over the Pd/Fe_3O_4 catalyst, in which the time-dependent concentration evolutions of nitrate, nitrite, and ammonium and the solution pH changes are presented. At the first 15 min of the nitrate reduction, the nitrate concentration dropped quickly. With the progress of the reaction, the speed of nitrate concentration decrease then slowed down. Correspondingly, the solution pH value initially increased fast and rate of the increase gradually slowed down. The ammonium concentration followed a similar trend. The nitrite concentration, however, was always very low (close to zero) during the whole reduction process. The maximum nitrite concentration (0.0048 mM) was found after 30 min reaction, and no nitrite was detected when the reaction time was 1 h and over. After 2 h reaction, the solution pH increased from 7.0 to 11.3, the nitrate concentration dropped from 1.61 mM to 0.157 mM ($X_{NO_3^-}$ was 90.25%), and the ammonium concentration increased from zero to 1.31 mM ($S_{NH_4^+}$ was 81.37%).

The complete disappearance of nitrite in the nitrate reduction experiment suggests that its reduction might be faster than the reduction of nitrate in this process so the concentration of the intermediate product nitrite could not build up in the denitrification process with the Pd/Fe_3O_4 catalyst. This observation is different from many reports on bimetallic catalysts [17,18,21,52–56] which showed high nitrite concentration in the treated water samples in the basic environment, and is very undesirable for water purification process because nitrite is more toxic than nitrate. Figure 4b shows the reduction result of nitrite over the Pd/Fe_3O_4 catalyst, in which the time-dependent concentration evolutions of nitrite, ammonium and the solution pH changes are presented. It is clear that it is much easier for nitrite to be reduced in the H_2/H_2O/catalyst system than nitrate. Under the current experimental conditions, the nitrite concentration dropped from 2.17 mM to 0.078 mM within just 10 min, and no nitrite could be detected after just 20 min. The faster reduction of nitrite indicates that it is more reactive in the H_2/H_2O/catalyst system than nitrate [57], and this observation is similar to some previous reports with the Pd/CeO_2 catalyst [33], the Pd/SnO_2 catalyst [47], and Pd/Cu bimetal catalyst [17].

It is well known that the nitrate could not be reduced only by the noble metal without a promoter in the denitrification process. In the Pd/Fe_3O_4 catalyst, it is clear that only Fe_3O_4 could serve as the promoter. Thus, nitrate should be reduced to nitrite firstly by Fe(II), while Fe(II) was oxidized to Fe(III) in the same time. Then, activated hydrogen could reduce Fe(III) to Fe(II), so the catalyst could always remain its composition. Fig. 4c and d shows the XRD diffraction pattern and the high-resolution XPS scan over Pd 3d on the Pd/Fe_3O_4 catalyst after its separation from the treated nitrate solution by an

Table 1
$X_{NO_3^-}$, $S_{NH_4^+}$ and maximum nitrite concentration at different pH.

Initial pH	4	6	7	8	10
$X_{NO_3^-}$ (%)	95.25	91.12	90.25	85.14	71.5
$S_{NH_4^+}$ (%)	86.12	85.14	81.51	78.14	66.7
$M_{NO_2^-}$ (mM)[a]	0.0052	0.0070	0.0048	0.0054	0.0046
Initial activity ($mmol_{Nitrate}\ min^{-1}\ g_{Pd}^{-1}$)	2.36	2.05	1.94	1.54	1.23

[a] *Note*: the maximum nitrite concentration in denitrification process.

external magnetic field, respectively, compared with that of the fresh Pd/Fe_3O_4 catalyst. It is clear that the Pd/Fe_3O_4 catalyst had the identical crystal structure and Pd maintained its metallic state before and after the catalytic denitrification process, which demonstrates that Pd/Fe_3O_4 did act as a catalyst in the denitrification process.

3.3. Effect of solution pH on activity and selectivity

The solution pH is an important parameter in the catalytic nitrate denitrification process. During this process, the solution pH increases when there is no pH control because hydroxyl ions are continuously produced by the reduction reaction. These hydroxyl ions may be adsorbed onto the active sites of the catalyst, which will then block the nitrate/nitrite reduction. The nitrate removal activity and the nitrogen formation selectivity will decrease with the increase of solution pH [20,21,52–56].

In this work, the solution pH was modulated in three different ways, and their effects on the catalytic denitrification activity and selectivity by the Pd/Fe_3O_4 catalyst were examined. Many previous reports [7,8,16,17,28–33] had demonstrated that the use of CO_2 as a buffer agent was an effective way to control the solution pH and increase the selectivity to N_2. So the use of CO_2 was firstly examined, and the reaction condition was kept the same with the nitrate reduction experiment except that 100 mL/min CO_2 was introduced into the reactor. However, it was found that $X_{NO_3^-}$ was dropped sharply from 90.25% to 30% after 2 h reaction and $S_{NH_4^+}$ was 70%. A byproduct of formic acid was found, which was produced by the reduction of CO_2 by activated H_2 in the presence of Pd/Fe_3O_4 catalyst, similar to the report of Stalder et al. on Pd/C catalyst [58]. So, a competitive reduction of CO_2 large hindered the nitrate reduction, and the use of CO_2 as the buffer agent could not enhance the catalytic nitrate reduction by Pd/Fe_3O_4.

Then, the initial nitrate solution pH value was adjusted to 4, 6, 7, 8 and 10, respectively, before the beginning of the catalytic nitrate reduction, and no pH adjustment was conducted in the process. Table 1 summarizes the initial activity, nitrate conversion, maximum nitrite concentration, and selectivity to ammonium at different pH after 2 h reaction. With the increase of the initial nitrate solution pH, $X_{NO_3^-}$ decreased constantly from 95.25% of pH 4 to 71.5% of pH 10. This observation is expected due to the electrostatic interaction of NO_3^- ions with the Pd/Fe_3O_4 surface. As demonstrated in Fig. 3a, the Pd/Fe_3O_4 surface is positively charged when the solution pH is below 5.8, while it is negatively charged when the solution pH is over 5.8 and the zeta-potential continues to decrease with the increase of the solution pH. The negatively charged NO_3^- ions could be attracted to the Pd/Fe_3O_4 surface when the solution pH was below 5.8 by the Coulomb force, while there could be repulsion between them when the solution pH was over 5.8 and the repulsion force increased with the increase of the solution pH. The repulsive electrostatic interaction made it difficult for NO_3^- ions to contact with active sites for nitrate reduction on Fe_3O_4 surface, which caused the decrease of $X_{NO_3^-}$. Interestingly, $S_{NH_4^+}$ decreased from 86.12% to 66.7% when the initial solution pH increased from 4 to 10, which is opposite to the previous reports on bimetallic catalysts [59–62].

We further examined the catalytic nitrate denitrification activity and selectivity by the Pd/Fe_3O_4 catalyst when the solution pH was controlled at a constant value during the reaction. For the comparison purpose, two pH values were chosen at 5.5 and 8.5, which represented attractive and repulsive interactions between NO_3^- ions and the Pd/Fe_3O_4 surface, respectively. Fig. 5a and b shows the time-dependent concentration evolutions of nitrate and ammonium when the solution pH was controlled at 5.5 and 8.5, respectively. The nitrate reduction was completed within just 30 min for pH 5.5, while 2 h reaction time was needed for a complete nitrate reduction for pH 8.5. The initial activities for pH 5.5 and 8.5 were 3.11 and 2.18 $mmol_{Nitrate}\ min^{-1}\ g_{Pd}^{-1}$, respectively. As expected, the Pd/Fe_3O_4 catalyst is more active in the weak acid condition when pH is less than 5.8.

3.4. The proposed mechanism for high ammonium selectivity

In the catalytic nitrate denitrification process, two nitrogen-containing surface species must encounter each other during the

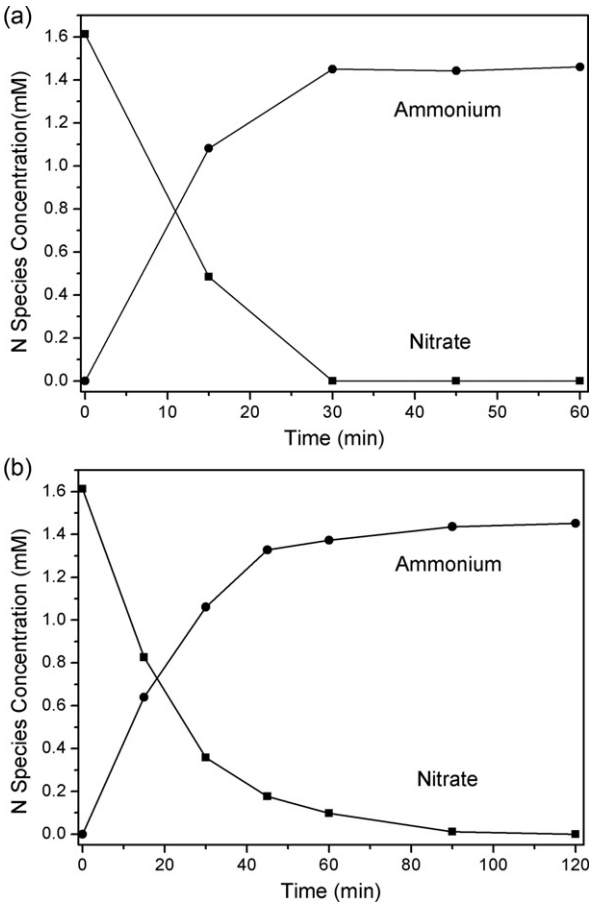

Fig. 5. The time-dependent concentration changes of nitrate and ammonium during the nitrate reduction process when the solution pH was controlled at (a) 5.5, and (b) 8.5.

hydrogenation to form N_2. Thus, the selectivity is controlled by the ratio of the surface coverage of N-species to reductant species (N: reductant ratio). Overreduction to NH_4^+ will occur when surface coverage of reductant increases, which decreases the N: reductant ratio and makes it more difficult for two nitrogen-containing surface species to encounter each other during the hydrogenation [16,17,26]. For bimetallic catalysts, nitrate is reduced to the intermediate product nitrite at the transition metal sites, and NO_2^- subsequently is reduced to N_2 or NH_4^+ by hydrogenation which mainly occurs on the noble metal sites [27,54]. Thus, the final product selectivity is determined mainly by the noble metal and NO_2^- hydrogenation [1,7,8,37,59], and it is generally reported that lower amount of ammonium was formed when the reaction was conducted under weak acid condition [53,62]. For bimetal catalysts, the hydroxyl ions produced during the reduction could be adsorbed onto the Pd and Pd-metal sites with the increase of solution pH, which inhibited the nitrite reduction on Pd sites [17,18,21,52–56] and sometimes even inhibited the nitrite reduction almost totally [55]. Thus, the nitrite concentration could be accumulated in the solution under alkaline conditions. In the present study, it was found that the main nitrate reduction product was ammonium no matter whether the catalytic denitrification was conducted in either acid or basic environment; nitrite could be completely reduced even in basic environment. These interesting observations are different from most previous reports on bimetallic catalysts [20–33], indicating that the reduction mechanism of the Pd/Fe_3O_4 catalyst may be quite different from those in the well-reported bimetallic catalysts.

In the present study, the nitrate was firstly reduced to nitrite on the surface of Fe_3O_4 by the Fe(II)/Fe(III) redox couple, and nitrite was subsequently reduced to nitrogen and ammonium. So the selectivity of the reduction product should also be determined by the nitrite reduction as in the bimetal catalyst. The high selectivity to ammonium suggests that the N: reductant ratio is not high in the Pd/Fe_3O_4 catalyst, which indicates that there should be large numbers of active sites on the Pd/Fe_3O_4 surface for nitrite reduction. During the denitrification process, hydroxyl ions produced by the reduction could be adsorbed onto Pd sites as seen in bimetal catalysts [52–56] and inhibited the nitrite reduction on Pd sites. The complete nitrite reduction by the Pd/Fe_3O_4 catalyst observed even in basic environment suggests that there must be active sites on Fe_3O_4 surface for the reduction of nitrite, which will also increase the number of active sites and decrease the N: reductant ratio so that the possibility of paring two nitrogen-containing surface species decreases and ammonium becomes the main product in this catalyst system.

Two series of experiments were designed in the present study to validate this mechanism hypothesis. Fig. 6a demonstrates the concentration evolutions when 100 ppm NO_3^- (1.61 mM) and 200 ppm NO_2^- (4.35 mM) ions co-existed under the catalytic denitrification by the Pd/Fe_3O_4 catalyst. The initial solution pH was adjusted to 10, because hydroxyl ions could be adsorbed onto Pd sites to inhibit the nitrite reduction on Pd sites under basic condition. The result demonstrated clearly that the reduction of nitrate was totally suppressed when a high concentration of nitrite co-existed in the reaction solution. Only when the nitrite reduction was almost completed and the nitrite concentration was near zero, the reduction of nitrate could begin. This observation clearly demonstrated that the nitrate and nitrite reduction could occur on the same sites, which should be the active sites on the surface of Fe_3O_4 for nitrate reduction to nitrite. Nitrite is known as a stronger oxidant than nitrate [53,63], so co-existing nitrite could suppress the nitrate reduction. Fig. 6b demonstrates the concentration evolutions of NO_2^- (200 ppm) ions under the catalytic denitrification by the Pd/Fe_3O_4 catalyst with the initial solution pH at 10, compared with that of NO_2^- with co-existing NO_3^- (100 ppm) under the same

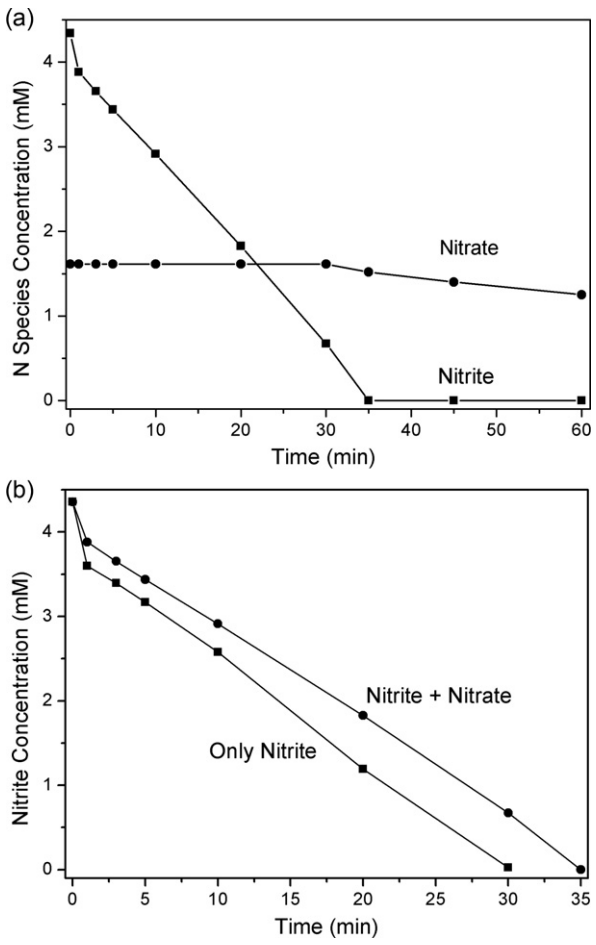

Fig. 6. (a) The time-dependent concentration changes of nitrate and nitrite during the reduction process when they co-existed in the reaction solution. (b) The time-dependent concentration changes of nitrite during the reduction process with and without co-existing nitrate.

reaction conditions. When there were co-existed NO_3^- ions, the nitrite reduction was slowed down, indicating that co-existing NO_3^- ions could also affect the nitrite reduction because some active sites for nitrite reduction could also be occupied by nitrate.

The NO_3^-/NO_2^- adsorptions on the Pd/Fe_3O_4 catalyst were examined with 1 mg/L nitrate, 1 mg/L nitrite, and coexisted 1 mg/L nitrate and 1 mg/L nitrite, respectively, without the presence of hydrogen. The pH value of these three solutions was ~7.0, and the Pd/Fe_3O_4 catalyst concentration was 0.5 g/L. The adsorption was conducted with continuous mechanical stirring and under N_2 atmosphere. After being stirred for 6 h, 10 mL sample was withdrawn for the analysis of remaining nitrate/nitrite. Table 2 shows the adsorption experiment results. The adsorption percentages of the nitrate and nitrite are 15.74% and 39.35%, respectively, when they exist separately. When nitrate and nitrite coexist, the adsorption percentages of nitrate and nitrite both decrease. The nitrate adsorption percentage drops from 15.74% to 7.14%, representing

Table 2
Adsorption rate of the nitrate and nitrite on Pd/Fe_3O_4 catalyst.

Adsorption species	Nitrate	Nitrite	Coexisted nitrate and nitrite	
			Nitrate	Nitrite
Initial concentration (mg/L)	1.06	1.08	1.02	1.01
Final concentration (mg/L)	0.8932	0.6550	0.9471	0.6740
Adsorption percentage (%)	15.74	39.35	7.14	32.27

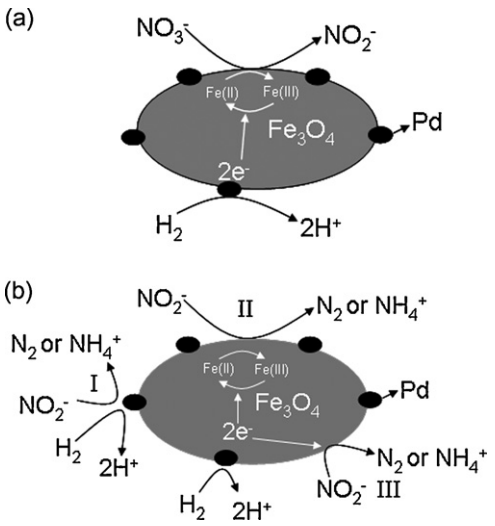

Fig. 7. Schematic illustrations of (a) nitrate and (b) nitrite deduction processes with the Pd/Fe_3O_4 catalyst.

a decrease of ~54.64%. The nitrite adsorption percentage, however, only falls from 39.35% to 32.27%, representing a decrease of ~17.99%. The adsorption experiment data indicates that there is also competitive adsorption between nitrate and nitrite, and their coexistence has a larger suppressing effect on the nitrate adsorption.

Thus, these two series of experiments clearly demonstrate that there are two kinds of active sites for nitrite reduction in the Pd/Fe_3O_4 catalyst. Besides the well known Pd sites, there are active sites on Fe_3O_4 surface that could also adsorb and reduce nitrite. It had been demonstrated in the previous reports that Fe(II) could be oxidized by nitrite under some conditions [64–66]. Thus, it could be concluded that nitrite may be reduced by Fe(II) on the surface of the Fe_3O_4 in the presence of Pd. After being oxidized to Fe(III) by nitrite, Fe(III) could subsequently be reduced to Fe(II) by activated hydrogen as expected for nitrate reduction. Fig. 7a and b schematically describes the nitrate and nitrite reduction processes with the Pd/Fe_3O_4 catalyst, respectively. Because the active sites on the Fe_3O_4 surface increase the density of active sites for nitrite reduction, it is more difficult for two nitrogen-containing surface species to encounter each other to form N_2. Moreover, the good electrical conductivity of Fe_3O_4 could facilitate the flow of electrons dissociated from hydrogen at accessible Pd sites as the following formula describes [67]:

$$H_2 \xleftrightarrow{Pd} 2H_{ads} \xleftrightarrow{Pd} 2H^+ + 2e^- \quad (5)$$

Thus, it is easy for electrons to flow towards Fe_3O_4 surface, which increases the surface reductants and also favors the formation of ammonium [51,67].

4. Conclusions

In this study, a novel magnetite supported monometallic Pd denitrification catalyst Pd/Fe_3O_4 was synthesized by a co-precipitation process followed with the reduction in pure hydrogen at 453 K. The Pd/Fe_3O_4 catalyst demonstrated a fast denitrification performance in water solution, especially when the solution pH was controlled at weak acidic condition (pH < 5.8). It was found that nitrite in the solution could be completely reduced by the Pd/Fe_3O_4 catalyst even under basic condition, which is very desirable for water purification purpose. Fe_3O_4 was found to play multifunctional roles in this catalyst system, and a different reduction mechanism from those in the bimetallic catalysts was found in the Pd/Fe_3O_4 catalyst. Besides its roles as the catalyst support and an ideal magnetic separation medium owing to its superparamagnetism, Fe_3O_4 was a good promoter for nitrate reduction, and could also provide active sites for nitrite reduction. Due to the large amount of active sites on the Pd/Fe_3O_4 catalyst and the good conductivity of Fe_3O_4, the N: reductant ratio was not high and the formation of ammonium was favored. Although the main product in the present study is the undesirable NH_4^+, its effective reduction of nitrite under alkaline condition and easy separation/recycling make Pd/Fe_3O_4 a potential catalyst for the denitrification application. A subsequent step, such as break-point chlorination with the addition of NaClO, could be easily added to oxidize the formed ammonium to N_2 and remove it from water to solve this issue. Future work will be conducted to further examine the intermediate products in this process, and explore the reaction mechanism in more details.

Acknowledgments

This study was supported by the National Basic Research Program of China (grant no. 2006CB601201), the Knowledge Innovation Program of Chinese Academy of Sciences (grant no. Y0N5711171), the Knowledge Innovation Program of Institute of Metal Research (grant no. Y0N5A111A1), and the Youth Innovation Promotion Association, Chinese Academy of Sciences (grant no. Y2N5711171).

References

[1] F. Epron, Journal of Catalysis 198 (2001) 309–318.
[2] A. Pintar, J. Batista, Catalysis Today 53 (1999) 35–50.
[3] N. Barrabes, A. Dafinov, F. Medina, J.E. Sueiras, Catalysis Today 149 (2010) 341–347.
[4] J.H. Choi, W.S. Shin, S.J. Choi, Y.H. Kim, Environmental Technology 30 (2009) 939–946.
[5] I. Mikami, Applied Catalysis B: Environmental 44 (2003) 79–86.
[6] R.F. Spalding, M.E. Exner, Journal of Environment Quality 22 (1993) 392–402.
[7] K. Nakamura, Y. Yoshida, I. Mikami, T. Okuhara, Applied Catalysis B: Environmental 65 (2006) 31–36.
[8] O.S.G.P. Soares, J.J.M. Órfão, M.F.R. Pereira, Catalysis Letters 126 (2008) 253–260.
[9] World Health Organization, Guidelines for Drinking-water Quality: Incorporating First and Second Addendum. vol. 1. Recommendations, 3rd ed., WHO Press, Geneva, 2008.
[10] J. Grimm, D. Bessarabov, R. Sanderson, Desalination 115 (1998) 285–294.
[11] F. Hell, J. Lahnsteiner, H. Frischherz, G. Baumgartner, Desalination 117 (1998) 173–180.
[12] E. Korngold, Water, Air, and Soil Pollution 2 (1973) 15–22.
[13] V. Mateju, S. Cizinska, J. Krejci, T. Janoch, Enzyme and Microbial Technology 14 (1992) 170–183.
[14] J.C. Fanning, Coordination Chemistry Reviews 199 (2000) 159–179.
[15] A. Pintar, J. Batista, J. Levec, T. Kajiuchi, Applied Catalysis B: Environmental 11 (1996) 81–98.
[16] U. Prüsse, K.D. Vorlop, Journal of Molecular Catalysis A: Chemical 173 (2001) 313–328.
[17] K.A. Guy, H. Xu, J.C. Yang, C.J. Werth, J.R. Shapley, Journal of Physical Chemistry C 113 (2009) 8177–8185.
[18] F. Gauthard, Journal of Catalysis 220 (2003) 182–191.
[19] U. Matatov Meytal, M. Sheintuch, Catalysis Today 102–103 (2005) 121–127.
[20] K.D. Vorlop, T. Tacke, Chemie Ingenieur Technik 61 (1989) 836–837.
[21] Y. Sakamoto, M. Kanno, T. Okuhara, Y. Kamiya, Catalysis Letters 125 (2008) 392–395.
[22] G. Strukul, F. Pinna, M. Marella, L. Meregalli, M. Tomaselli, Catalysis Today 27 (1996) 209–214.
[23] A. Pintar, J. Batista, J. Levec, Catalysis Today 66 (2001) 503–510.
[24] F.A. Marchesini, L.B. Gutierrez, C.A. Querini, E.E. Miró, Chemical Engineering Journal 159 (2010) 203–211.
[25] O. Ilinich, Catalysis Today 82 (2003) 49–56.
[26] O.M. Ilinitch, F.P. Cuperus, L.V. Nosova, E.N. Gribov, Catalysis Today 56 (2000) 137–145.
[27] A.E. Palomares, J.G. Prato, F. Márquez, A. Corma, Applied Catalysis B: Environmental 41 (2003) 3–13.
[28] A.E. Palomares, C. Franch, A. Corma, Catalysis Today 149 (2010) 348–351.
[29] G. Mendow, F.A. Marchesini, E.E. Miroï, C.A. Querini, Industrial and Engineering Chemistry Research 50 (2011) 1911–1920.
[30] A. Devadas, S. Vasudevan, F. Epron, Journal of Hazardous Materials 185 (2011) 1412–1417.

[31] J. Sa, T. Berger, K. Fottinger, A. Riss, J. Anderson, H. Vinek, Journal of Catalysis 234 (2005) 282–291.
[32] R. Gavagnin, L. Biasetto, F. Pinna, G. Strukul, Applied Catalysis B: Environmental 38 (2002) 91–99.
[33] F. Epron, F. Gauthard, J. Barbier, Journal of Catalysis 206 (2002) 363–367.
[34] H. Hu, Z. Wang, L. Pan, Journal of Alloys and Compounds 492 (2010) 656–661.
[35] S. Ordóñez, B.P. Vivas, F.V. Diez, Applied Catalysis B: Environmental 95 (2010) 288–296.
[36] G. Li, Z. Zhao, J. Liu, G. Jiang, Journal of Hazardous Materials 192 (2011) 277–283.
[37] H. Tian, J. Li, Q. Shen, H. Wang, Z. Hao, L. Zou, Q. Hu, Journal of Hazardous Materials 171 (2009) 459–464.
[38] B. Qiao, L. Liu, J. Zhang, Y. Deng, Journal of Catalysis 261 (2009) 241–244.
[39] J. Liu, B. Sun, J. Hu, Y. Pei, H. Li, M. Qiao, Journal of Catalysis 274 (2010) 287–295.
[40] O.S.G.P. Soares, J.J.M. Órfão, M.F.R. Pereira, Applied Catalysis B: Environmental 102 (2011) 424–432.
[41] S.C. Barret, B.T. Massalski, Structure of Metals, McGraw-Hill, New York, 1966.
[42] M. Brun, A. Berthet, J.C. Bertolini, Journal of Electron Spectroscopy 104 (1999) 55–60.
[43] D. Maity, S.N. Kale, R. Kaul Ghanekar, J.M. Xue, J. Ding, Journal of Magnetism and Magnetic Materials 321 (2009) 3093–3098.
[44] L. Xiao, J. Li, D.F. Brougham, E.K. Fox, N. Feliu, A. Bushmelev, A. Schmidt, N. Mertens, F. Kiessling, M. Valldor, B. Fadeel, S. Mathur, ACS Nano 5 (2011) 6315–6324.
[45] T. Yang, R. Brown, L. Kempel, P. Kofinas, Journal of Magnetism and Magnetic Materials 320 (2008) 2714–2720.
[46] A.H. Lu, E.L. Salabas, F. Schüth, Angewandte Chemie International Edition 46 (2007) 1222–1244.
[47] M. Daarino, Applied Catalysis B: Environmental 53 (2004) 161–168.
[48] M.A. Keane, Journal of Chemical Technology and Biotechnology 80 (2005) 1211–1222.
[49] M.A. Keane, Journal of the Chemical Society, Faraday Transactions 93 (1997) 2001–2007.
[50] G. Yuan, M.A. Keane, Chemical Engineering Science 58 (2003) 257–267.
[51] J.K. Chinthaginjala, J.H. Bitter, L. Lefferts, Applied Catalysis A-General 383 (2010) 24–32.
[52] Y. Sakamoto, K. Nakata, Y. Kamiya, T. Okuhara, Chemistry Letters 33 (2004) 908–909.
[53] L. Lemaignen, C. Tong, V. Begon, R. Burch, D. Chadwick, Catalysis Today 75 (2002) 43–48.
[54] André F L., Catalysis Today 53 (1999) 23–34.
[55] Y. Sakamoto, Y. Kamiya, T. Okuhara, Journal of Molecular Catalysis A: Chemical 250 (2006) 80–86.
[56] A. Pintar, J. Batista, Journal of Hazardous Materials 149 (2007) 387–398.
[57] J. Sá, J.A. Anderson, Applied Catalysis B: Environmental 77 (2008) 409–417.
[58] C.J. Stalder, S. Chao, D.P. Summers, M.S. Wrighton, Journal of the American Chemical Society 105 (1983) 6318–6320.
[59] J. Sá, H. Vinek, Applied Catalysis B: Environmental 57 (2005) 247–256.
[60] A. Pintar, G. Berčič, J. Levec, AlChE Journal 44 (1998) 2280–3392.
[61] O. Soares, J.M.J. Orfao, J. Ruiz-Martinez, J. Silvestre-Albero, A. Sepulveda-Escribano, M.F.R. Pereira, Chemical Engineering Journal 165 (2010) 78–88.
[62] Y. Yoshinaga, Journal of Catalysis 207 (2002) 37–45.
[63] A.J. Coby, F.W. Picardal, Applied and Environment Microbiology 71 (2005) 5267–5274.
[64] D. Mishra, J. Farrell, Environmental Science and Technology 39 (2004) 645–650.
[65] V. Ernstsen, Clays and Clay Minerals 44 (1996) 599–608.
[66] Y.H. Huang, T.C. Zhang, Chemosphere 64 (2006) 937–943.
[67] J.K. Chinthaginjala, L. Lefferts, Applied Catalysis B: Environmental 101 (2010) 144–149.